Ab initio Ehrenfest dynamics

Xiaosong Li, John C. Tully, H. Bernhard Schlegel, and Michael J. Frisch

Citation: J. Chem. Phys. **123**, 084106 (2005); doi: 10.1063/1.2008258
View online: http://dx.doi.org/10.1063/1.2008258
View Table of Contents: http://jcp.aip.org/resource/1/JCPSA6/v123/i8
Published by the American Institute of Physics.

Ab initio Ehrenfest dynamics

Xiaosong Li[a)]
Department of Chemistry, University of Washington, Seattle, Washington 98195

John C. Tully[b)]
Department of Chemistry, Yale University, New Haven, Connecticut 06520

H. Bernhard Schlegel
Department of Chemistry, Wayne State University, Detroit, Michigan 48202

Michael J. Frisch
Gaussian, Inc., Wallingford, Connecticut 06492

(Received 21 April 2005; accepted 5 July 2005; published online 30 August 2005)

We present an *ab initio* direct Ehrenfest dynamics scheme using a three time-step integrator. The three different time steps are implemented with nuclear velocity Verlet, nuclear-position-coupled midpoint Fock integrator, and time-dependent Hartree-Fock with a modified midpoint and unitary transformation algorithm. The computational cost of the *ab initio* direct Ehrenfest dynamics presented here is found to be only a factor of 2–4 larger than that of Born-Oppenheimer (BO) dynamics. As an example, we compute the vibration of the NaCl molecule and the intramolecular torsional motion of $H_2C{=}NH_2^+$ by Ehrenfest dynamics compared with BO dynamics. For the vibration of NaCl with an initial kinetic energy of 1.16 eV, Ehrenfest dynamics converges to BO dynamics with the same vibrational frequency. The intramolecular rotation of $H_2C{=}NH_2^+$ produces significant electronic excitation in the Ehrenfest trajectory. The amount of nonadiabaticity, suggested by the amplitude of the coherent progression of the excited and ground electronic states, is observed to be directly related to the strength of the electron-nuclear coupling. Such nonadiabaticity is seen to have a significant effect on the dynamics compared with the adiabatic approximation. © *2005 American Institute of Physics*. [DOI: 10.1063/1.2008258]

I. INTRODUCTION

Classical trajectory calculations[1] are often able to provide greater insight into the dynamics of reactions than do stationary analysis of molecular properties. The Born-Oppenheimer (BO) and extended Lagrangian (EL) trajectories[2–4]are founded on the assumption that a single electronic potential surface governs the dynamics. Such adiabatic approaches are widely used in investigations of reactions on ground-state surfaces. A major limitation of adiabatic trajectories is that they are not applicable to reactions involving nonadiabatic electronic processes, i.e., multiple potential-energy surfaces. Proper incorporation of the electronic response is crucial for describing a host of dynamical processes, including laser-induced chemistry, dynamics at metal or semiconductor surfaces, and electron transfer in molecular, biological, interfacial, or electrochemical systems. The two most widely used approaches to account for nonadiabatic effects are the surface-hopping method with its many variants,[5,6] and the Ehrenfest method implemented here. The surface-hopping approach extends the Born-Oppenheimer framework to the nonadiabatic regime by allowing stochastic electronic transitions subject to a time- and momenta-dependent hopping probability. A direct *ab initio* dynamics algorithm using surface hopping has been implemented using complete active-space self-consistent-field (CASSCF) wave functions.[7] When the system consists of many atoms, this approach, however, becomes rather demanding computationally because an explicit computation of adiabatic time-dependent excited-state wave functions is required in surface hopping.

The exact treatment of electronic nonadiabaticity can be obtained in principle by solving the time-dependent Schrödinger equation (TDSE) simultaneously for both electrons and nuclei. However, explicit numerical integration of the full TDSE is computationally prohibitive, except for very small systems. An approximation to the expansion of TDSE over all the excited states is the reduction to a single Slater determinant, as exemplified by the time-dependent Hartree-Fock (TDHF)[8–10] and time-dependent density-functional theory (TDDFT).[11] The TDHF or TDDFT avoids explicit computations of excited states and represents the wave function as a coherent superposition state. As a result, all chemical properties such as potential, force, and electron density are calculated as mean expectation values. The propagation of classical trajectories for molecules represented by such a mean potential surface is often called Ehrenfest dynamics. Ehrenfest dynamics have been computed numerically in several applications.[5,8,12,13]

The integration of the Ehrenfest dynamics by a straightforward single time-step method is not efficient because the integration step size must be on the time scale of the elec-

[a)]Author to whom correspondence should be addressed. Electronic mail: li@chem.washington.edu
[b)]Electronic mail: john.tully@yale.edu

tronic motion, usually more than an order of magnitude shorter than that of the nuclear motion. Micha and coworkers have developed the *relax-and-drive* procedure with different time scales to propagate the coupled electronic and nuclear motions.[13–15] The *relax* step corresponds to an integration of the electronic TDHF equations at a fixed nuclear position. The *drive* step,

$$\Delta \boldsymbol{P} = \boldsymbol{U} \cdot \boldsymbol{\Delta}' \cdot \boldsymbol{U}^{\dagger}, \tag{1}$$

where $\boldsymbol{\Delta}' = \int \{[\mathbf{F}(t') - \mathbf{F}(t_k)], \mathbf{U} \cdot \mathbf{P}(t_k) \cdot \mathbf{U}^{\dagger}\} dt'$, comes from the effect of the motion of the nuclei on the integration of electronic degrees of freedom. It accounts for the change of the electron density, resulting from the change of the Fock operator, and indirectly couples the electronic degrees of freedom with nuclear motion through the Fock operator.

In this paper, we introduce an efficient *ab intio* direct Ehrenfest dynamics algorithm within the Hartree-Fock approximation. The energy, gradient, and molecular properties are computed "on the fly." A three-time-step integrator with nuclear velocity Verlet, nuclear-position-coupled midpoint Fock integrator, and time-dependent Hartree-Fock with a modified midpoint and unitary transformation algorithm is presented.

II. METHODOLOGY

We use the following notations and index conventions throughout this paper:

(1) x denotes atomic Cartesian coordinates.
(2) p denotes atomic momenta.
(3) $\boldsymbol{g}$ denotes the energy gradient (first derivative with respect to nuclear coordinates).
(4) χ denotes the atomic orbital (AO) basis (real values in this paper).
(5) ϕ denotes the molecular orbital.
(6) $\boldsymbol{S}$ denotes the overlap matrix, $S_{\mu\nu} = \langle \chi_\mu | \chi_\nu \rangle$.
(7) $\boldsymbol{P}'$ and $\boldsymbol{P}$ denote the complex density matrices in the AO basis and orthonormal basis, respectively.
(8) $\boldsymbol{h}'(x)$ and $\boldsymbol{h}(x)$ denote the one-electron matrices calculated at atomic coordinates x,

$$h'_{\mu,\nu}(x) = \left\langle \chi_\mu \left| -\frac{1}{2}\nabla^2 - \sum_A \frac{Z_A}{|r - r_A|} \right| \chi_\nu \right\rangle,$$

in the AO basis and orthonormal basis, respectively.
(9) $\boldsymbol{G}'(x, \boldsymbol{P}')$ and $\boldsymbol{G}(x, \boldsymbol{P}')$ denote the two-electron matrices calculated with density $\boldsymbol{P}'$ at atomic coordinates x,

$$\begin{aligned} G'^{\alpha}_{\mu,\nu}(x, \boldsymbol{P}') = \sum_{\lambda,\sigma} P'^{\alpha}_{\lambda\sigma} \Bigg\{ & \left[\chi_\mu(1)\chi_\nu(1) \left| \frac{1}{r_{12}} \right| \chi_\lambda(2)\chi_\sigma(2) \right] \\ & - \left[\chi_\mu(1)\chi_\sigma(1) \left| \frac{1}{r_{12}} \right| \chi_\lambda(2)\chi_\nu(2) \right] \Bigg\} \\ & + \sum_{\lambda,\sigma} P'^{\beta}_{\lambda\sigma} \left[\chi_\mu(1)\chi_\nu(1) \left| \frac{1}{r_{12}} \right| \chi_\lambda(2)\chi_\sigma(2) \right], \end{aligned}$$

in the AO basis and orthonormal basis, respectively.
(10) $\boldsymbol{F}'$ and $\boldsymbol{F}$ denote the complex Fock matrices, $F'_{\mu\nu} = h'_{\mu\nu} + G'_{\mu\nu}(x, \boldsymbol{P}')$, in the AO basis and orthonormal basis, respectively.
(11) A, B are atomic indices.
(12) μ, ν are atomic orbital indices.
(13) $k, k+1$ are time indices.

In an orthonormal basis, the TDHF equation for the density matrix can be written as

$$i\frac{\partial \boldsymbol{P}}{\partial t} = \boldsymbol{F}\boldsymbol{P} - \boldsymbol{P}\boldsymbol{F}. \tag{2}$$

In general, the basis functions are not orthonormal, hence the overlap matrix is not the identity. This basis can always be orthonormalized by means of Löwdin or Cholesky transformation methods. The density matrix and the Fock matrix are transformed from the AO basis ($\boldsymbol{P}'$ and $\boldsymbol{F}'$) into an orthonormal basis ($\boldsymbol{P}$ and $\boldsymbol{F}$) by a transformation matrix $\boldsymbol{V}$:

$$\boldsymbol{P} = \boldsymbol{V} \cdot \boldsymbol{P}' \cdot \boldsymbol{V}^T \quad \text{and} \quad \boldsymbol{F} = \boldsymbol{V}^{-T} \cdot \boldsymbol{F}' \cdot \boldsymbol{V}^{-1}. \tag{3}$$

In the Löwdin orthonormalization method, $\boldsymbol{V} = \boldsymbol{S}^{1/2}$; in the Cholesky method, the upper triangular $\boldsymbol{V}$ is obtained by the decomposition $\boldsymbol{S} = \boldsymbol{V}^T\boldsymbol{V}$.

When an atom-centered basis set is used to represent the density, additional terms arise because of the time dependence of the position of the basis functions.[3,13,15] These spurious coupling terms can be eliminated through the use of traveling atom functions, $|\xi\rangle = T_m(\boldsymbol{r}, t)|\chi\rangle$.[3,13,15] The atom translation factor is given by

$$T_m(\boldsymbol{r}, t) = \exp\left\{ \frac{i \cdot m_e}{\hbar} \left[\boldsymbol{\nu}_m(t) \cdot \boldsymbol{r} - \int dt \cdot \frac{\nu^2 t}{2} \right] \right\}. \tag{4}$$

When the nuclear velocities are small, the atom translation factors will be near unity. As a first approximation, they are omitted in the present study.

A. Time-dependent Hartree-Fock electronic dynamics

In a recent paper,[10] we introduced the integration of the time-dependent Hartree-Fock theory using a modified midpoint and unitary transformation TDHF (MMUT-TDHF) algorithm to study the electron optical response in intense laser fields. A comparison with a direct numerical integration of TDSE indicates that TDHF is capable of realistically simulating some aspects of nonadiabatic electronic dynamics.

In the MMUT-TDHF algorithm, the Fock matrix at time t_k is expressed in its eigenspace,

$$\boldsymbol{C}^{\dagger}(t_k) \cdot \boldsymbol{F}(t_k) \cdot \boldsymbol{C}(t_k) = \boldsymbol{\varepsilon}(t_k). \tag{5}$$

A unitary transformation matrix $\boldsymbol{U}(t_k)$, which is written in terms of the eigenvectors $\boldsymbol{C}(t_k)$ and eigenvalues $\varepsilon(t_k)$ of the Fock matrix, is used to propagate the density matrix from time t_{k-1} to t_{k+1}.

$$\boldsymbol{P}_{k+1} = \boldsymbol{U}(t_k) \cdot \boldsymbol{P}(t_{k-1}) \cdot \boldsymbol{U}^{\dagger}(t_k), \tag{6}$$

$$\begin{aligned} \boldsymbol{U}(t_k) &= \exp[i \cdot 2\Delta t_e \cdot \boldsymbol{F}(t_k)] \\ &= \boldsymbol{C}(t_k) \cdot \exp[i \cdot 2\Delta t_e \cdot \boldsymbol{\varepsilon}(t_k)] \cdot \boldsymbol{C}^{\dagger}(t_k). \end{aligned} \tag{7}$$

The MMUT-TDHF method takes into account linear changes in the density during the time step by computing the Fock matrix at the midpoint of the step. The time step for integrating the MMUT-TDHF equations will be denoted as Δt_e.

Equation (6) is exact only for a constant Fock matrix. Even if the nuclei do not move, the Fock matrix is still time dependent since the electron density $\boldsymbol{P}$ is time dependent. Because of this, the time step Δt_e has to be small enough so that the MMUT-TDHF step is accurate. However, the integrals used to construct the Fock matrix change very little on this time scale and can be kept constant for several Δt_e time steps.

B. Nuclear-position-coupled midpoint Fock integrator

The Fock matrix

$$\boldsymbol{F}' = \boldsymbol{h}'(x) + \boldsymbol{G}'(x,\boldsymbol{P}') \tag{8}$$

is a function of the nuclear coordinates and electron density. The MMUT-TDHF steps [Eqs. (5)–(7)] require a reconstruction of the Fock matrix from updates of the nuclear positions and electron density. Considering that the change of the nuclear coordinates is much slower than the change of the electronic wave function, it is reasonable to assume stationary nuclei for several MMUT-TDHF iterations before recalculating the integrals with the updated nuclear coordinates. We introduce a time step $\Delta t_{Ne} = m\Delta t_e$. The Fock matrix for the MMUT-TDHF step is built using the integrals calculated at the midpoint of the Δt_{Ne} time step, $t' + \Delta t_{Ne}/2$, and the instantaneous electron density matrix

$$\boldsymbol{F}'(t) = \boldsymbol{h}'[x(t' + \Delta t_{Ne}/2)] + \boldsymbol{G}'[x(t' + \Delta t_{Ne}/2), \boldsymbol{P}'(t')]. \tag{9}$$

This nuclear-position-coupled midpoint Fock algorithm can be further understood in analogy to the nuclear velocity Verlet (Sec. II C) if we assign the Fock operator and electron density the roles of nuclear momentum and position. In the nuclear velocity Verlet method, the momentum at half time is used to move nuclei from $x(t'_k)$ to $x(t'_{k+1})$, while in the midpoint Fock algorithm the Fock matrix constructed with nuclear position at half time propagates the electron density from $\boldsymbol{P}(t'_k)$ to $\boldsymbol{P}(t'_{k+1})$. The time step for two consecutive updates of nuclear coordinates for constructing the Fock matrix and electron-nuclear coupling will be denoted as Δt_{Ne}. The change of nuclear position affects electronic degrees of freedom at a much shorter time scale than do changes in the nuclear gradient. It will be computationally efficient to embed several updates of nuclear coordinates for constructing the Fock matrix and electron-nuclear coupling between two consecutive calculations of the gradient, mainly because computing the derivative of the two-electron term $\partial \boldsymbol{G}'(x,\boldsymbol{P})/\partial x_A$ is about four times as expensive as computing just $\boldsymbol{G}'(\boldsymbol{P})$. We introduce a time step $\Delta t_N = n\Delta t_{Ne}$ for the interval between the recalculation of the energy gradient.

C. Classical nuclear dynamics and energy derivative

The classical equations of motion, $M_A \ddot{x}_A = -\partial E/\partial x_A$, can be solved numerically with a number of standard methods. In this paper, velocity Verlet[16] is used to integrate the nuclear motion moving on a mean potential of a superposition state,

$$p_A(t_{k+1/2}) = p_A(t_k) - \tfrac{1}{2} g_A(t_k) \cdot \Delta t_N, \tag{10}$$

$$x_A(t_{k+1}) = x_A(t_k) + \frac{p_A(t_{k+1/2})}{M_A} \cdot \Delta t_N, \tag{11}$$

$$p_A(t_{k+1}) = p_A(t_{k+1/2}) - \tfrac{1}{2} g_A(t_{k+1}) \cdot \Delta t_N. \tag{12}$$

The mean force comes from the calculation of the first derivative of the energy with respect to nuclear coordinates, using the TDHF-propagated wave function. Since $[\boldsymbol{F},\boldsymbol{P}] \neq 0$, the derivative is different than for Born-Oppenheimer dynamics.[4]

$$\frac{\partial E}{\partial x_A} = \frac{\partial \mathrm{v}_{NN}}{\partial x_A} + \mathrm{Tr}\left[\frac{d\boldsymbol{h}'}{dx_A}\boldsymbol{P}' + \frac{1}{2}\left.\frac{\partial \boldsymbol{G}'}{\partial x_A}\right|_{P'} \boldsymbol{P}' \right] - \mathrm{Tr}\left[\boldsymbol{F}'\boldsymbol{V}^{-1}\frac{d\boldsymbol{V}}{dx_A}\boldsymbol{P}' + \boldsymbol{P}'\frac{d\boldsymbol{V}}{dx_A}\boldsymbol{V}^{-1}\boldsymbol{F}' \right]. \tag{13}$$

The derivatives of the transformation matrix $\boldsymbol{V}$ must be computed explicitly. In the case of the Löwdin orthonormalization,

$$\frac{d\boldsymbol{V}}{dx_A} = \sum_{i,j} \boldsymbol{s}_i \frac{1}{\sigma_i^{1/2} + \sigma_j^{1/2}} \left(\boldsymbol{s}_i^T \frac{d\boldsymbol{S}'}{dx_A} \boldsymbol{s}_j \right) \boldsymbol{s}_j^T, \tag{14}$$

where $\boldsymbol{s}_i$ and σ_i are, respectively, the ith eigenvector and eigenvalue of the overlap matrix $\boldsymbol{S}'$; in the case of the Cholesky transformation,[4]

$$\begin{aligned} \left[\frac{d\boldsymbol{V}}{dx_A}\boldsymbol{V}^{-1} \right]_{\mu,\nu} &= \left[\boldsymbol{V}^{-T}\frac{d\boldsymbol{V}^T}{dx_A} \right]_{\nu,\mu} \\ &= \left(\boldsymbol{V}^{-T}\frac{d\boldsymbol{S}'}{dx_A}\boldsymbol{V}^{-1} \right)_{\mu,\nu} \quad \text{when } \mu < \nu, \\ &= \frac{1}{2}\left(\boldsymbol{V}^{-T}\frac{d\boldsymbol{S}'}{dx_A}\boldsymbol{V}^{-1} \right)_{\mu,\nu} \quad \text{when } \mu = \nu, \\ &= 0 \quad \text{when } \mu > \nu. \end{aligned} \tag{15}$$

Note that the gradient is always real due to the fact that both $\boldsymbol{F}$ and $\boldsymbol{P}$ are Hermitian and the basis functions are real.

D. The overall Ehrenfest integration scheme and accuracy

The three time steps, $\Delta t_N, \Delta t_{Ne}$, and Δt_e are associated with nuclear velocity Verlet (Sec. II C), nuclear-position-coupled midpoint Fock integrator (Sec. II B) and MMUT-TDHF (Sec. II A) integrators, respectively. The idea is to propagate the nuclei using the velocity Verlet with steps of Δt_N assuming that the change in the gradient is small during the step. The Δt_N step is divided into n smaller steps Δt_{Ne}. The various integrals are recomputed for each step so that they can be used in the construction of the Fock matrix. Since the density changes more rapidly than do the integrals, the Δt_{Ne} step is divided into m smaller steps of Δt_e. The density is propagated using the MMUT-TDHF method using steps of Δt_e. As illustrated in Fig. 1, several midpoint Fock steps are embedded in one nuclear velocity Verlet step. To drive the electron density, several MMUT-TDHF steps are carried out within one nuclear-position-coupled midpoint Fock step.

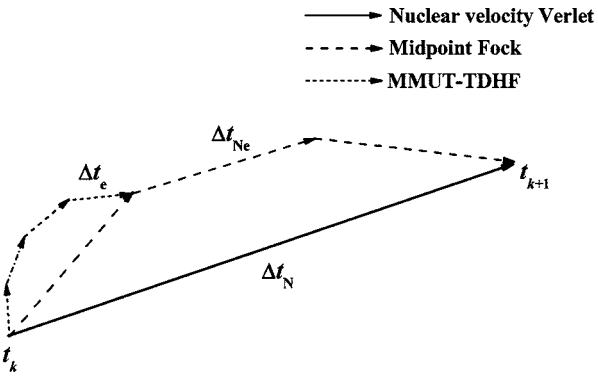

$\Delta t_{Ne} = \Delta t_N / n,\ \Delta t_e = \Delta t_{Ne} / m$

Do k
  $t_k = t_{k-1} + \Delta t_N$
  Calculate $g(t_k)$ at $x(t_k)$ [eq. 13]
  Calculate $p(t_{k+1/2})$ and $x(t_{k+1})$ [eq. 10, 11]
  Do j = 1, n
    $t' = t_k + (j-1)\ \Delta t_{Ne}$
    $\mathbf{x}(t' + ½\ \Delta t_{Ne}) = \mathbf{x}(t_k) + (t' + ½\ \Delta t_{Ne})\ p(t_{k+1/2})/M$
    Calculate $\mathbf{h}'$, $(\mu\nu||\lambda\sigma)$, $\mathbf{S}$ and $\mathbf{V} = \mathbf{S}^{1/2}$
    Do i = 1, m
      $\tau = t' + (i-1)\ \Delta t_e$
      $\mathbf{P}'(\tau) = \mathbf{V}^{-1}\ \mathbf{P}(\tau)\ \mathbf{V}^{-T}$
      Form $\mathbf{F}'(\tau)$ using $\mathbf{P}'(\tau)$ and the current integrals
      $\mathbf{F}(\tau) = \mathbf{V}^{-1}\ \mathbf{F}'(\tau)\ \mathbf{V}^{-T},\ \mathbf{U} = \exp(i\ 2\ \Delta t_e\ \mathbf{F}(\tau))$
      $\mathbf{P}(\tau+\Delta t_e) = \mathbf{U}\ \mathbf{P}(\tau-\Delta t_e)\ \mathbf{U}^T$
      End Do
    End Do
  End Do

FIG. 1. Three-time-scale integration scheme for Ehrenfest dynamics.

It is instructive to examine the computational cost of the midpoint Fock integration scheme described above. The expensive steps in Ehrenfest dynamics consist of computations of the energy first derivative with respect to the nuclear position $g(T_g)$, the MMUT-TDHF step (T_{TDHF}), the two-electron integrals (T_{2e}), the one-electron integrals (T_{1e}), and the overlap matrix $\boldsymbol{S}(T_{\boldsymbol{S}})$. Note that T_{TDHF} includes the cost of forming and diagonalizing the Fock matrix. For small- to medium-sized systems, the CPU times are usually in the order $T_g > T_{\mathrm{TDHF}} \approx T_{2e} > T_{1e} \approx T_{\boldsymbol{S}}$. The cost of Ehrenfest dynamics using only one time step for M integration steps of Δt_e can be estimated as

$$T_{\mathrm{Ehrenfest}} = M(T_{\boldsymbol{S}} + T_{1e} + T_{2e} + T_{\mathrm{TDHF}} + T_g). \tag{16}$$

By comparison, the cost of the midpoint Fock algorithm is approximately

$$T_{\text{mid-Fock-Ehrenfest}} = M \cdot \left(\frac{\Delta t_e}{\Delta t_{Ne}} \cdot (T_{\boldsymbol{S}} + T_{1e} + T_{2e}) + T_{\mathrm{TDHF}} + \frac{\Delta t_e}{\Delta t_N} \cdot T_g \right). \tag{17}$$

The cost of the nuclear-position-dependent electron integration is reduced by $\Delta t_e / \Delta t_{Ne}$, and the evaluation of the gradient is reduced by $\Delta t_e / \Delta t_N$. In anticipation of applications to larger systems, two-electron integrals are computed in a direct[17] fashion in this paper.

The overall accuracy of the three-time-step Ehrenfest dynamics lies in the error of each individual integrator and their intrinsic connections. In Ehrenfest dynamics, nuclei are treated as classical particles and nuclear operators do not appear in the total Hamiltonian. Therefore, the integration of nuclear trajectory is an independent problem of solving the Newton's equations. A single velocity Verlet step for classical dynamics has been shown to be accurate up to the third order (see Ref. 18 for details). Nuclear terms appear in the electron Hamiltonian as instantaneous attractive potentials, resulting in the general time-dependent Hartree-Fock equation for the electron wave function,

$$i\frac{\partial \phi(x,t)}{\partial t} = \hat{F}\phi(x,t)$$

and

$$\phi(x, t + \Delta t_e) = e^{-i\Delta t \hat{F}}\phi(x,t). \tag{18}$$

Equation (18) is a general problem of factorizing exponential operators. The midpoint Fock is equivalent to the widely used second-order three-split-operator symmetric decomposition of the time-dependent Schrödinger equation,[19,20] where the Fock operator is split into nuclear-position-dependent and nuclear-position-independent parts. Such decomposition is second order for a single step and has been shown to approach a third-order accuracy with increasing number of splitting or iterations, $\Delta t_N = n\Delta t_{Ne}$ and $n \to \infty$.[19] In this paper, a second operator splitting is used to decompose the nuclear-position-independent Fock operator into $\hat{F}$ and $\Delta\hat{F}$, where $\hat{F}$ is a constant within Δt_e and updated after Δt_e with $\Delta\hat{F}$ resulting from the change of electron density. The modified midpoint TDHF is applied to integrate the second level of splitting. The MMUT-TDHF is a second-order method as well and approaches a third-order accuracy when $m \to \infty$, where $\Delta t_{Ne} = m\Delta t_e$.

Figure 2 illustrates numerical analyses of energy errors for the midpoint Fock and MMUT-TDHF integrators, respectively. We choose the vibrational dynamics of NaCl, starting with a converged wave function and an initial kinetic energy of 4.6 eV, integrated up to one velocity Verlet step for this numerical analysis. The error for the midpoint Fock algorithm is an accumulative error, in reference to the BO energy at the end of one velocity Verlet step, computed at the end of a nuclear step $\Delta t_N = 0.5$ fs with a constant $\Delta t_e = 0.0001$ fs for integrating the TDHF. Similarly, the error for the MMUT-TDHF is an accumulative energy error in a single nuclear step $\Delta t_N = 0.5$ fs, $\Delta t_{Ne} = 0.25$ fs. Both integrators exhibit $O(\Delta t^{2-3})$ growth of errors with respect to the step size. At the step-size limit, the MMUT-TDHF still introduces about 1.59×10^{-4} a.u. energy error [Fig. 2(b)]. This additional error can be corrected by using multiple midpoint Fock steps within one nuclear step. Figure 2(a) shows that the midpoint Fock method corrects the energy error, approaching the complete error correction at the step-size limit. It is clear that the use of several midpoint Fock steps is able to reduce the overall energy error without introducing too much additional computational cost.

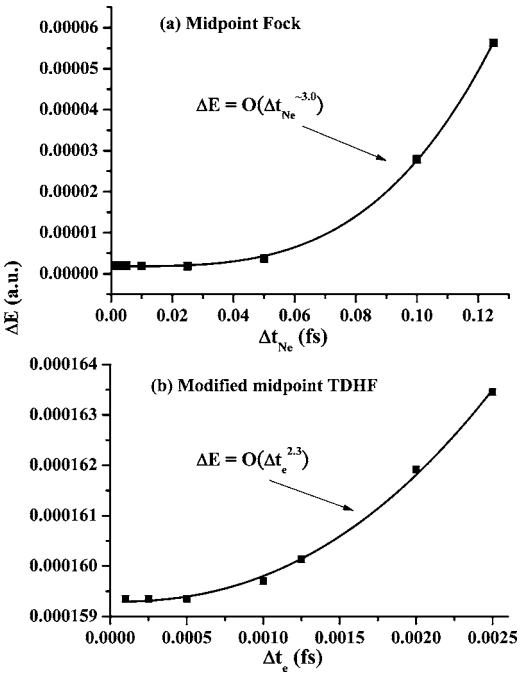

FIG. 2. Accuracy analyses for (a) midpoint Fock (Δt_N=0.5 fs, Δt_e =0.0001 fs), and (b) modified midpoint TDHF integrators (Δt_N =0.5 fs, Δt_{Ne}=0.25 fs).

III. BENCHMARK AND DISCUSSION

To illustrate the implementation and properties of the midpoint Fock Ehrenfest algorithm discussed above, we have considered two examples: the vibration of NaCl and the internal rotation of $H_2C{=}NH_2^+$. Electron integrals are computed using the development version of the GAUSSIAN package.[21] Natural population analysis (NPA) is used to analyze atomic properties on the fly. All the timing data presented here were collected on an Intel Pentium-4 3.2-GHz single-processor workstation.

A. The vibration of NaCl

Figure 3 illustrates the vibration of NaCl computed with the direct Born-Oppenheimer (BO) and the midpoint Fock Ehrenfest approaches. Calculations were carried out at the HF or TDHF level of theory using the 3-21G all-electron basis. The dynamics with midpoint Fock integrator are tested using several sets of time steps. Trajectories were started at the NaCl equilibrium geometry ($R_{\mathrm{Na-Cl}}$=2.4210 Å) with an initial vibrational kinetic energy of 1.16 eV. It is readily apparent from Fig. 3 that the vibrational frequencies by the Ehrenfest approach are almost the same as the BO trajectory with less than 0.1% difference. It also indicates that the vibration of NaCl with an initial kinetic energy of 1.16 eV is nearly adiabatic. For the *ab initio* Ehrenfest dynamics, the midpoint Fock method is computationally very efficient. The self-consistent convergence of the wave function at each step in the BO trajectory is replaced with iterations to propagate $\boldsymbol{P}$ according to the time-dependent Hartree-Fock theory. For the system considered here, integrating one direct Ehrenfest trajectory up to 300 fs with Δt_N=0.5, Δt_{Ne}=0.05, and Δt_e =0.005 fs in the "direct" fashion takes only twice as many total iterations as converging the self-consistent field, and therefore twice of the CPU time of one BO trajectory with Δt_N=0.5 fs.

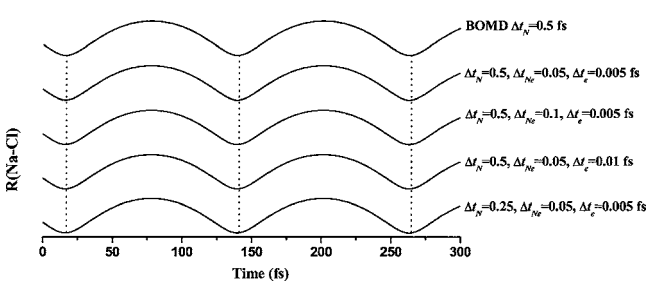

FIG. 3. Vibration of NaCl computed using the Born-Oppenheimer approach and the Ehrenfest dynamics with different integration time steps ($R_{\min}$ =1.97 Å and $R_{\max}$=3.42 Å).

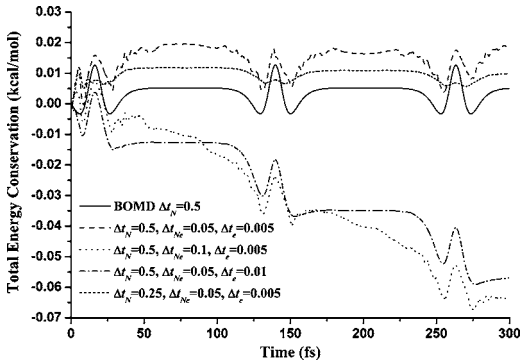

FIG. 4. Comparison of total-energy conservation for various sets of time steps using the Ehrenfest dynamics.

Figure 4 compares the total-energy conservation for various sets of time steps: (a) BO trajectory with Δt_N=0.5 fs; (b) Ehrenfest with Δt_N=0.5, Δt_{Ne}=0.05, and Δt_e=0.005 fs; (c) Ehrenfest with Δt_N=0.5, Δt_{Ne}=0.1, and Δt_e=0.005 fs; (d) Ehrenfest with Δt_N=0.5, Δt_{Ne}=0.05, and Δt_e=0.01 fs, and (e) Ehrenfest with Δt_N=0.25, Δt_{Ne}=0.05, and Δt_e=0.005 fs. The total energy by the Ehrenfest approach is conserved to 0.023 and 0.012 kcal/mol for (b) and (e), respectively, compared with 0.013 kcal/mol for the BO trajectory with Δt_N =0.5 fs (a). For an energy conservation that is comparable to the BO trajectory, the Ehrenfest trajectory as (e) in Fig. 4 is about four times as expensive as the BO trajectory. If the midpoint Fock step Δt_{Ne} or the MMUT-TDHF step Δt_e is too big as in the (c) and (d) cases, a systematic error is readily noticeable even though the total energy is still conserved very well over a short interval. When an appropriate set of time steps is used as in the (b) and (e) case, the time evolution of the energy conservation by the Ehrenfest dynamics is comparable to the Born-Oppenheimer dynamics, indicating an excellent time reversibility.

B. The rotation of $H_2C{=}NH_2^+$

A 180° internal rotation about a covalent double bond involves the breaking and reformation of the relatively rigid π bond. During the rotation, excited states often participate in the dynamics as a result of the strong electron-nuclear coupling. The rotational barrier of $H_2C{=}NH_2^+$ is formed by the avoided crossing of two rotational potential curves. In many cases, such rotational potential curves may cross

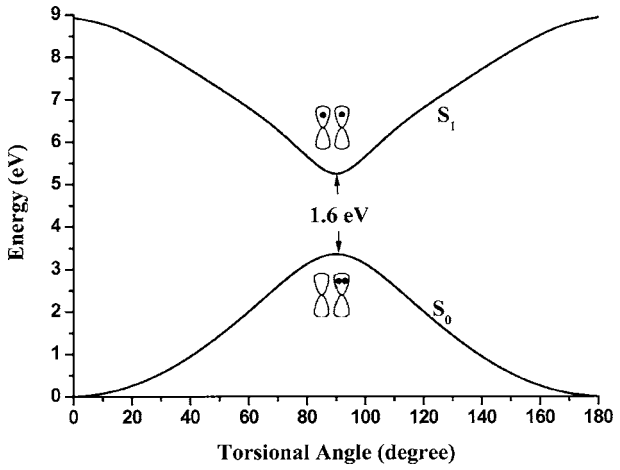

FIG. 5. Adiabatic potential-energy curves of the ground and first excited states of $H_2C{=}NH_2^+$ computed using linear-response TDHF.

through a conical intersection. Figure 5 shows the adiabatic potential-energy curves of the ground (S_0) and first excited states (S_1) from a rigid rotation; i.e., the torsional angle is the only geometric variable. The $\pi \rightarrow \pi^*$ excited state is calculated using linear response TDHF.[22] The ground-state (S_0) potential curve corresponds to the inhomogeneous breakage of the π bond, leading to the $H_2C^+ - NH_2$ configuration at the top of the barrier. The potential-energy surface of the first excited state (S_1) comes from the homogenous bond breakage forming a $H_2C^{\cdot} - {}^{\cdot}N^+H_2$ diradical at the torsional angle of 90°. The smallest energy gap between two curves is about 1.6 eV.

Figure 6 illustrates the dynamics of the $H_2C{=}NH_2^+$ internal rotation about the double bond starting from the planar equilibrium geometry and with several different torsional kinetic energies. The natural charges of the NH_2 group are plotted as a function of the torsional angle. When excited states participate in the dynamics, nuclear gradients often change more drastically than for the adiabatic case. In order to conserve the energy better, nuclear time steps have to be smaller than those without much nonadiabaticity as in Sec. III A. The total energy is conserved to better than 0.08, 0.09, and 0.15 kcal/mol in Fig. 6(a), 6(b), and 6(b), respectively, with $\Delta t_N = 0.1, \Delta t_{Ne} = 0.01$, and $\Delta t_e = 0.001$ fs. The BO trajectories propagate strictly on the S_0 state as required by the adiabatic BO approximation. In the avoided crossing region, the strong electron-nuclear coupling can result in an electronic nonadiabatic transition so that molecules can be found in the excited state. Such a phenomenon cannot be simulated by the adiabatic BO molecular dynamics. By contrast, the Ehrenfest dynamics implicitly incorporates the electron-nuclear coupling, and therefore is able to account for the nonadiabaticity in the simulation. Near the avoided crossing region, the Ehrenfest trajectories begin to deviate from the adiabatic behavior, apparently due to the electron-nuclear-coupling-induced electronic transition. The resulting coherent superposition of excited and ground states leads to the oscillation of charge. The strength of the nonadiabatic behavior, as indicated by the amplitude of the coherent oscillation or deviation from the BO dynamics, depends systematically on the initial nuclear momentum, with higher nuclear kinetic energy resulting in a stronger nonadiabatic behavior. A more detailed investigation of the electronic nonadiabatic behavior will be discussed in a subsequent paper.

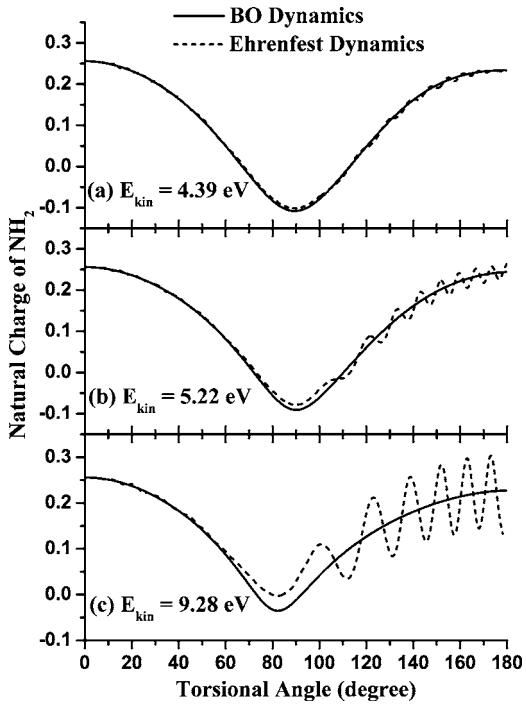

FIG. 6. Dynamics of $H_2C{=}NH_2^+$ internal rotation about the double bond with different initial torsional kinetic energies.

IV. CONCLUSION

Ehrenfest dynamics propagates classical nuclei on a mean potential surface corresponding to an electronic superposition state. We have developed a three-time-scale algorithm with nuclear velocity Verlet, nuclear-position-coupled midpoint Fock integrator, and time-dependent Hartree-Fock using modified midpoint and unitary transformation for *ab initio* direct Ehrenfest dynamics. In particular, the coupled electronic and nuclear motions are propagated by the nuclear-position-coupled midpoint Fock method.

The Ehrenfest method presented in this paper is computationally practical and able to account for nonadiabatic electronic excitations within a superposition state framework. The computational cost of Ehrenfest dynamics is only 2–4 times of that for the BO dynamics. The energy conservation and time reversibility are well maintained in the midpoint Fock Ehrenfest dynamics. The algorithm introduced here can be extended to the Ehrenfest dynamics within the time-dependent density-functional theory (TDDFT).

ACKNOWLEDGMENTS

This work was supported by grants from the National Science Foundation (CHE0314208 and CHE0131157).

[1] D. L. Bunker, *Methods in Computational Physics* (Academic Press, New York, 1971), Vol. 10, p. 287; L. M. Raff and D. L. Thompson, *Theory of Chemical Reaction Dynamics* (CRC, Boca Raton, 1985); *Advances in Classical Trajectory Methods*, edited by W. L. Hase (JAI, Greenwich, 1992), Vol. 1; D. L. Thompson, in *Encyclopedia of Computational Chem-*

istry, edited by P. v. R. Schleyer, N. L. Allinger, T. Clark, J. Gasteiger, P. A. Kollman, H. F. Schaefer III, and P. R. Schreiner (Wiley, Chichester, New York, 1998), p. 3059.
[2] K. Bolton, W. L. Hase, and G. H. Peslherbe, in *Modern Methods for Multidimensional Dynamics Computation in Chemistry*, edited by D. L. Thompson (World Scientific, Singapore, 1998); R. Car and M. Parrinello, Phys. Rev. Lett. **55**, 2471 (1985); M. E. Tuckerman, P. J. Ungar, T. von Rosenvinge, and M. L. Klein, J. Phys. Chem. **100**, 12878 (1996); M. C. Payne, M. P. Teter, D. C. Allan, T. A. Arias, and J. D. Joannopoulos, Rev. Mod. Phys. **64**, 1045 (1992); D. K. Remler and P. A. Madden, Mol. Phys. **70**, 921 (1990); D. Marx and J. Hutter, edited by J. Grotendorst (John von Neumann Institute for Computing, Julich, 2000), Vol. 1, p. 301; J. M. Millam, V. Bakken, W. Chen, W. L. Hase, and H. B. Schlegel, J. Chem. Phys. **111**, 3800 (1999).
[3] E. Deumens, A. Diz, R. Longo, and Y. Ohrn, Rev. Mod. Phys. **66**, 917 (1994); J. B. Delos, *ibid.* **53**, 287 (1981).
[4] H. B. Schlegel, J. M. Millam, S. S. Iyengar, G. A. Voth, A. D. Daniels, G. E. Scuseria, and M. J. Frisch, J. Chem. Phys. **114**, 9758 (2001).
[5] P. V. Parandekar and J. C. Tully, J. Chem. Phys. **122** 094102 (2005).
[6] B. Space and D. F. Coker, J. Chem. Phys. **94**, 1976 (1991); G. Parlant and E. A. Gislason, *ibid.* **91**, 4416 (1989); N. C. Blais, D. G. Truhlar, and C. A. Mead, J. Chem. Phys. **89**, 6204 (1988); C. W. Eaker, *ibid.* **87**, 4532 (1987); R. E. Cline and P. G. Wolynes, *ibid.* **86**, 3836 (1987); J. R. Stine and J. T. Muckerman, J. Chem. Phys. **91**, 459 (1987); N. C. Blais and D. G. Truhlar, J. Chem. Phys. **79**, 1334 (1983); J. R. Stine and J. T. Muckerman, *ibid.* **68**, 185 (1978); **65**, 3975 (1976); W. H. Miller and T. F. George, *ibid.* **56**, 5637 (1972); J. C. Tully and R. K. Preston, *ibid.* **55**, 562 (1971); J. C. Tully, *ibid.* **93**, 1061 (1990); J. C. Tully, in *Dynamics of Molecular Collisions*, edited by W. H. Miller (Plenum, New York, 1976), Vol. 2, p. 217.
[7] A. Sanchez-Galvez, P. Hunt, M. A. Robb, M. Olivucci, T. Vreven, and H. B. Schlegel, J. Am. Chem. Soc. **122**, 2911 (2000); T. Vreven, F. Bernardi, M. Garavelli, M. Olivucci, M. A. Robb, and H. B. Schlegel, *ibid.* **119**, 12687 (1997); G. A. Worth, P. Hunt, and M. A. Robb, J. Phys. Chem. A **107**, 621 (2003).
[8] K. C. Kulander, Phys. Rev. A **36**, 2726 (1987); K. C. Kulander, K. R. S. Devi, and S. E. Koonin, *ibid.* **25**, 2968 (1982).
[9] G. H. Chen and S. Mukamel, J. Chem. Phys. **103**, 9355 (1995).
[10] X. Li, S. M. Smith, A. N. Markevitch, D. A. Romanov, R. J. Levis, and H. B. Schlegel, Phys. Chem. Chem. Phys. **7**, 233 (2005).
[11] E. Runge and E. K. U. Gross, Phys. Rev. Lett. **52**, 997 (1984); B. X. Xu and A. K. Rajagopal, Phys. Rev. A **31**, 2682 (1985); A. K. Dhara and S. K. Ghosh, *ibid.* **35**, 442 (1987); V. Chernyak and S. Mukamel, *ibid.* **52**, 3601 (1995); J. Chem. Phys. **112**, 3572 (2000).
[12] S. I. Sawada, A. Nitzan, and H. Metiu, Phys. Rev. B **32**, 851 (1985); Z. Kirson, R. B. Gerber, A. Nitzan, and M. A. Ratner, Surf. Sci. **137**, 527 (1984); D. A. Micha, J. Chem. Phys. **78**, 7138 (1983); A. D. McLachlan, Mol. Phys. **8**, 39 (1964); M. J. Field, J. Chem. Phys. **96**, 4583 (1992); K. Runge and D. A. Micha, Phys. Rev. A **53**, 1388 (1996); K. Runge, D. A. Micha, and E. Q. Feng, Int. J. Quantum Chem. Suppl., **24**, 781 (1990).
[13] D. A. Micha, J. Phys. Chem. A **103**, 7562 (1999); D. A. Micha and K. Runge, Phys. Rev. A **50**, 322 (1994).
[14] D. A. Micha, *Advances In Quantum Chemistry* (Academic Press, New York, 1999), Vol. 35, p. 317.
[15] E. Q. Feng, D. A. Micha, and K. Runge, Int. J. Quantum Chem. **40**, 545 (1991).
[16] L. Verlet, Phys. Rev. **159**, 98 (1967).
[17] S. Saebo and J. Almlof, Chem. Phys. Lett. **154**, 83 (1989); J. Almlof, K. Faegri, and K. Korsell, J. Comput. Chem. **3**, 385 (1982).
[18] A. K. Mazur, J. Comput. Phys. **136**, 354 (1997).
[19] Q. Sheng, IMA J. Numer. Anal. **9**, 199 (1989); S. Z. Burstein and A. A. Mirin, J. Comput. Phys. **5**, 547 (1970); A. D. Bandrauk and H. Shen, Chem. Phys. Lett. **176**, 428 (1991); A. D. Bandrauk and H. Shen, J. Chem. Phys. **99**, 1185 (1993).
[20] K. C. Kulander, Phys. Rev. A **38**, 778 (1988); M. Suzuki, J. Math. Phys. **26**, 601 (1985).
[21] M. J. Frisch, G. W. Trucks, H. B. Schlegel *et al.*, GAUSSIAN, Development Version (Wallingford, CT, 2004).
[22] R. E. Stratmann, G. E. Scuseria, and M. J. Frisch, J. Chem. Phys. **109**, 8218 (1998).